Band structures of a dipolar Bose-Einstein condensate in one-dimensional lattices

YuanYao Lin,[1] Ray-Kuang Lee,[1] Yee-Mou Kao,[2] and Tsin-Fu Jiang[3,*]
[1]*Institute of Photonics Technologies, National Tsing-Hua University, Hsinchu 300, Taiwan*
[2]*Department of Physics, National Changhua University of Education, Changhua 500, Taiwan*
[3]*Institute of Physics, National Chiao Tung University, Hsinchu 300, Taiwan*
(Received 14 February 2008; published 25 August 2008)

We derive the effective Gross-Pitaevskii equation for a cigar-shaped dipolar Bose-Einstein condensate in one-dimensional lattices and investigate the band structures numerically. Due to the anisotropic and the long-ranged dipole-dipole interaction in addition to the known contact interaction, we elucidate the possibility of modifying the band structures by changing the alignment of the dipoles with the axial direction. With the considerations of the transverse parts and the practical physical parameters of a cigar-shaped trap, we show the possibility to stabilize an attractive condensate simply by adjusting the orientation angle of dipoles. Some interesting Bloch waves at several particle current densities are identified for possible experimental observations.

DOI: 10.1103/PhysRevA.78.023629 PACS number(s): 03.75.Lm, 05.30.Jp

I. INTRODUCTION

The Bose-Einstein condensate (BEC) in an optical lattice has provided a versatile and controllable platform to study the condensed-matter-like properties by the atomic quantum gases [1]. As electrons in a crystal lattice, matter waves in laser-induced optical lattices have many similar but ubiquitous interesting features due to the nonlinear atom-atom interactions in BECs. Bloch waves with discrete eigenenergy are the stationary solutions for BEC in periodic potentials. The resulting band structures are identified by the Brillouin zones. With the nonlinear mean-field Gross-Pitaevskii equation, the swallow-tailed loop structure at the boundary of the Brillouin zone was first predicted by a simple two-state model [2]. Later on, an exact solution of such loop behaviors in the band structure was found for a particular kind of one-dimensional lattice [3,4], and was further studied numerically by a detailed many-mode expansion method [5,6]. The atomic band structures are related to the dynamics and stability of the condensates. The new property has attracted intensive investigations, including the nonlinear Landau-Zener tunneling [2,7], the Bloch oscillation [8,9], and the stability of Bloch waves [6,10].

In 2005, a new species of dipolar BEC was realized in addition to the alkali-metal atoms BEC systems since the first realization in 1995. This dipolar system uses chromium atoms, ^{52}Cr. Each chromium atom has a magnetic dipole moment of 6 Bohr magneton which is larger than that of the alkaline atom [11–14]. More recently, ^{52}Cr BEC was produced with an all-optical method [15]. For the dipolar BEC, there is then an extra dipole-dipole interaction between atoms in addition to the known contact interaction in the BECs of alkali-metal atoms. The dipole-dipole interaction is anisotropic and long-ranged. So, there are new tunable parameters from this interaction. There are renewed interests in the dipolar BEC due to the dipole force. Namely, an unusual property of double-peak order parameter for the dipolar BEC under certain environments was demonstrated [16]; and the effects of the dipolar interaction to the quantum phase transition temperature was also explored [17]. The stability, ground state, and excitations of the dipolar BEC in a trap potential were already investigated in the literature [18–20]. It was found that the Luttinger-liquid phase persists for a wide range of density in one-dimensioanl dipolar gas [21]. The solidlike to liquidlike phase change of the one-dimensional dipolar system ground state with respect to the linear density by the quantum Monte Carlo method was shown [22]. The signature of one-dimensional dipolar gas in the Super-Tonks-Girardeau regime was studied [23]. The ground state phase diagram of the two-dimensional dipolar gas was also investigated [24]. Applying the Bose-Hubbard model to the system of dipolar BEC in a two-dimensional optical lattice, the possibility of several quantum phases for the ground state with different aspect ratios was elucidated [25]. An extension to dipolar spinor BEC was also explored recently [26]. More interestingly, a novel structure of dipolar bosons in a planar array of one-dimensional tubes was proposed [27].

The goal of this paper is to investigate the band structures of the dipolar BEC in a quasi-one-dimensional optical lattice. As shown in Ref. [25], in the case of extreme quantum regime, there are several possible phases for the ground state for dipolar Bosons in optical lattice. Instead of using the Bose-Hubbard model with long-range force, mean-field theory is applied here as the cases of nondipolar bosons in lattice and our system parameters are within the range of superfluid phase. The number density of atoms we considered will be quite large and without significant fluctuations. In such a scenario, even though the effects of the transverse confinement could wash out some of the ground states, but effectively with the regime of a mean-field approach one only obtains a modified one-dimensional Gross-Pitaevskii equation with coefficients depending on the geometry of the ground state. Instead of using the ideal pure one-dimensional lattice model [2–6], in this work we use practical physical parameters of a cigar-shaped trap and take into account the effects of transverse parts. As mentioned above, with the dipolar potential, the effects of the spatial distribution of the

*tfjiang@faculty.nctu.edu.tw

atoms must be treated with special attentions. Our calculation follows the method of many-mode expansion in Refs. [5,6] and the convergent results are shown. We found that the transverse part modifies the coupling constant, and the dipole-dipole interaction can be reduced to an effective contact term with adjustable parameter γ, which is the angle between the aligned dipoles and the axial direction. Interestingly, the band structures can be tuned by adjusting the angle γ. This is a special property of the band structures for the dipolar BEC in optical lattices; and it is also possible to adjust the angle γ such that a BEC with attractive interaction can be stable without collapse.

Besides the ultracold atomic systems, artificial periodic structures with the modulation in the refractive index in a Kerr-type nonlinear material, known as nonlinear photonic crystals, also share the same knowledge of such loop structures. For example, experimental observation of photonic Bloch oscillations and Zener tunneling were reported in a photorefractive material with configurable two-dimensional square lattices [28]. In terms of nonlinear wave packets, periodic potentials of optical lattices in a condensate also supported the unique solution, called gap solitons [29]. Gap solitons have attracted a great deal of attention due to their controllable interaction and robust evolution uninhibited by collapse. The swallow-tail structures are related to the split even- and odd-numbered periodic soliton arrays [6,30]. Since the band structures determine the dispersion relation for optical waves, the results in this work also provide useful information for the studies of wave packets inside *nonlocal* nonlinear photonic crystals, such as their mobilities and interactions [31,32].

The rest of the paper is organized as follows: In Sec. II, the formulation of a dipolar BEC in quasi-one-dimensional optical lattices was derived from the three-dimensional Gross-Pitaevskii equation with a cigar-shaped trap. In Sec. III, we describe the method of solution based on many-mode expansions; and the results with several sets of physical parameters are presented in Sec. IV, especially some interesting cases of Bloch waves with zero particle current density. Finally, the discussion and conclusions are presented.

II. FORMULATION

We consider the mean-field equation for a system of N aligned dipolar atoms in a quasi-one-dimensional lattice described by the time-independent Gross-Pitaevskii equation,

$$\mu\Psi(\vec{r}) = \left[-\frac{\hbar^2}{2m}\nabla^2 + V_{trap} + Ng_s|\Psi(\vec{r})|^2 + Ng_d \int d^3r' V_d(\vec{r},\vec{r}')|\Psi(\vec{r}')|^2 \right]\Psi(\vec{r}). \quad (1)$$

Here $V_{trap}=\frac{1}{2}m\omega_\perp^2(x^2+y^2)+V_0\sin^2(\frac{\pi z}{d})$, $g_s=4\pi\hbar^2 a/m$, $g_d=\mu_0\mu_m^2/4\pi$, m is the atomic mass, a is the scattering length, and μ_m is the atomic magnetic dipole moment. Note that in a cigar-shaped trap, the trap frequency for the axial direction is much smaller than the transverse frequency $\omega_\perp$ and is thus neglected. More specifically, we take the recently realized ^{52}Cr dipolar BEC system as a model case. With millions of BEC atoms in a cigar-shaped trap modulated by hundreds of lattice sites and the dipoles aligned in the direction $\hat{p}$, besides the constant g_d, the dipole-dipole interaction potential in the above equation is written as

$$V_d(\vec{r},\vec{r}') = \frac{1-3|\hat{p}\cdot\hat{e}_{rr'}|^2}{|\vec{r}-\vec{r}'|^3},$$

where $\hat{e}_{rr'}=\frac{\vec{r}-\vec{r}'}{|\vec{r}-\vec{r}'|}$ is the unit vector. Note that there is no contact term in the dipole-dipole potential V_d. Because under the mean-field theory, an atom has been modeled as a hard sphere with radius of the scattering length and the overlap of two atoms is not considered.

In the cigar-shaped trap, we may assume the transverse part of the solution stays in the ground state of the harmonic potential, that is,

$$\psi(\vec{r}) = \phi_g(x,y)\phi(z), \quad (2)$$

where $\phi_g(x,y)=e^{-(x^2+y^2)/2L_w^2}/\sqrt{\pi L_w^2}$ is the ground state of harmonic potential in the x-y directions, and $L_w=\sqrt{\hbar/m\omega_\perp}$ is the length scale of the transverse wave function. We approximate the z-direction wave function in the Bloch form:

$$\phi(z) = \phi_B(z)e^{ikz}, \quad (3)$$

where $\phi_B(z+d)=\phi_B(z)$ is a periodic function for the lattice constant d. The independent wave number k lies in the first Brillouin zone, $[-\pi/d,\pi/d]$. We use the scaled units $\hbar=m=1$ unless otherwise stated. For hundreds of lattice sites, the above assumptions are valid and used often [33,34]. We label the site index as $j=-M,-M+1,\ldots,-2,-1,0,1,2,\ldots,M-1,M$. Then the Fourier expansion is used due to the periodicity in the Bloch function:

$$\phi_B(z) = \sum_{\nu=-\nu_M}^{\nu_M} c_\nu e^{i\nu(2\pi z/d)}, \quad (4)$$

where all the mode coefficients c_ν are real numbers [5]; and with the normalization condition,

$$\int_{-[M+(1/2)]d}^{[M+(1/2)d} |\phi(z)|^2 dz = (2M+1)\int_{\text{one site}} |\phi_B(z)|^2 dz = (2M+1)d\left[\sum_\nu c_\nu^2\right] = 1, \quad (5)$$

one can obtain a condition for all the coefficients. Usually, only few modes in the expansion are enough to give convergent results. For the illustrations demonstrated later, we coin the expansions with $M=1,2,3,\ldots$ as the $3-,5-,7-,\ldots$ mode approximation, respectively.

We multiply Eq. (1) with $\phi_g(x,y)$ and integrate over x and y directions to obtain

$$(\mu-\hbar\omega_\perp)\phi(z) = \left[-\frac{\hbar^2}{2m}\frac{d^2}{dz^2} + V_0\sin^2\left(\frac{\pi z}{d}\right) + \frac{Ng_s}{2\pi L_w^2}|\phi(z)|^2 + Ng_d\int dxdy\,\phi_g(x,y)^2\int V_d(\vec{r},\vec{r}') \times|\Psi(\vec{r}')|^2 d^3r' \right]\phi(z). \quad (6)$$

We can see that the transverse part modifies the coupling constant of the contact interaction term; but even with the approximation in the transverse part, the system is still hard to solve due to the nonlocal dipolar interaction. The treatment in the conjugate space [16] is applied to solve Eq. (6). We first define the nonlocal potential as

$$V_{\text{nonlocal}}(\vec{r}) = \int V_d(\vec{r},\vec{r'})|\Psi(\vec{r'})|^2 d^3r'. \tag{7}$$

Here the dipole-dipole interaction potential V_d depends on the relative position $\vec{r}-\vec{r'}$. Thus the above integral is in convolutional type. It can be calculated by inverse Fourier transform of the product of the Fourier transform of $|\Psi(\vec{r})|^2$ and $V_d(\vec{r})$. The Fourier transform of $V_d(\vec{r})$ is

$$\begin{aligned} U_d(\vec{q}) &= \int d^3r V_d(\vec{r}) e^{i\vec{q}\cdot\vec{r}} \\ &= -4\pi(1-3\cos^2\alpha)\left[\frac{\sin(qa)}{(qa)^3} - \frac{\cos(qa)}{(qa)^2}\right] \\ &\simeq -\frac{4\pi}{3}(1-3\cos^2\alpha), \end{aligned} \tag{8}$$

where α is the angle between the vector $\vec{q}$ and the aligned dipoles. The last form comes from the mean-field theory because the value of qa is small practically [16]. The density function in momentum space is defined as

$$\begin{aligned} n(\vec{q}) &= \int d^3r |\Psi(\vec{r})|^2 e^{i\vec{q}\cdot\vec{r}} \\ &\equiv \int dxdy\phi_g(x,y)^2 e^{i(q_1x+q_2y)} \int dz|\phi(z)|^2 e^{iq_3z} \\ &\equiv n_\perp(q_1,q_2)n_z(q_3), \end{aligned} \tag{9}$$

where with the transverse approximation, we have

$$n_\perp(q_1,q_2) = e^{-(L_w^2/4)(q_1^2+q_2^2)}. \tag{10}$$

Using the periodic property,

$$\int_{(j+1/2)d}^{(j+3/2)d} |\phi(z)|^2 e^{iq_3z} dz = e^{iq_3d} \int_{(j-1/2)d}^{(j+1/2)d} |\phi(z)|^2 e^{iq_3z} dz, \tag{11}$$

we find

$$n_z(q_3) = 2\sin\frac{(2M+1)q_3d}{2}\left[\frac{1}{(2M+1)q_3d} + \sum_{\mu,\nu;\mu\neq\nu} \frac{(-1)^{\mu+\nu}c_\mu c_\nu}{2\pi(\mu-\nu)/d+q_3}\right]. \tag{12}$$

Then, from the convolutional theorem, we have

$$V_{\text{nonlocal}}(\vec{r}) = \frac{1}{8\pi^3}\int d^3q U_d(\vec{q}) n(\vec{q}) e^{-i\vec{q}\cdot\vec{r}}. \tag{13}$$

In this way, we can define in Eq. (6) the effective axial potential as

$$V_{eff}(z) \equiv \int dxdy\phi_g(x,y)^2 V_{\text{nonlocal}}(\vec{r}). \tag{14}$$

After some reduction steps, we obtain

$$\begin{aligned} V_{eff}(z) &= \frac{-1}{6\pi^2}\int e^{-[(q_1^2+q_2^2)L_w^2/2]}(1-3\cos^2\alpha)n_z(q_3)e^{-iq_3z} \\ &\equiv V_1(z) + V_2(z), \end{aligned} \tag{15}$$

where we define

and

$$V_2(z) = \frac{1}{2\pi^2}\int e^{-[(q_1^2+q_2^2)L_w^2/2]} n_z(q_3)\cos^2\alpha e^{-iq_3z} d^3q. \tag{17}$$

The V_1 is easily worked out as

$$V_1(z) = -\frac{2}{3L_w^2}|\phi(z)|^2. \tag{18}$$

For $V_2(z)$, we need more manipulations. Due to the cylindrical symmetry, we can choose $\vec{p}=(\sin\gamma, 0, \cos\gamma)$ without loss of generality, where γ is the angle between the direction of dipoles and the z axis, i.e.,

$$\cos^2\alpha = (q_1\sin\gamma + q_3\cos\gamma)^2/(q_1^2+q_2^2+q_3^2).$$

We first integrate over (q_1,q_2) in polar coordinates, with $(q_1,q_2)=k(\cos\theta,\sin\theta)$, and obtain

$$\begin{aligned} &\int e^{[-(q_1^2+q_2^2)L_w^2/2]}\cos^2\alpha dq_1dq_2 \\ &= \pi\int_0^\infty e^{-(k^2L_w^2/2)}\frac{(k^2\sin^2\gamma + 2q_3^2\cos^2\gamma)}{k^2+q_3^2}kdk. \end{aligned} \tag{19}$$

The final approximated format for $V_2(z)$ is derived in the following:

$$\begin{aligned} V_2(z) &= \frac{1}{2\pi}\int e^{-iq_3z} n_z(q_3)[I(q_3)\sin^2\gamma + 2J(q_3)\cos^2\gamma]dq_3 \\ &\sim \sin^2\gamma|\phi(z)|^2/L_w^2, \end{aligned} \tag{20}$$

where we define $I(q_3)$ and $J(q_3)$ as

$$I(q_3) \equiv \int_0^\infty e^{-(k^2L_w^2/2)}\frac{k^2}{k^2+q_3^2}kdk = \frac{1}{L_w^2} + \frac{q_3^2}{2}e^{q_3^2L_w^2/2}E_i\left[-\frac{q_3^2L_w^2}{2}\right], \tag{21}$$

$$J(q_3) \equiv \int_0^\infty e^{-(k^2L_w^2/2)}\frac{q_3^2}{k^2+q_3^2}kdk = \frac{1}{L_w^2} - I(q_3), \tag{22}$$

with the exponential integral,

$$E_i[-x] = -\int_x^\infty \frac{e^{-t}}{t}dt \quad \text{with } x>0. \tag{23}$$

We can see that for small value of q_3, $I(q_3)\sim 1/L_w^2$ and $J(q_3)\sim 0$; while for a large value of q_3, $I(q_3)\to 2/(q_3^2L_w^4)$

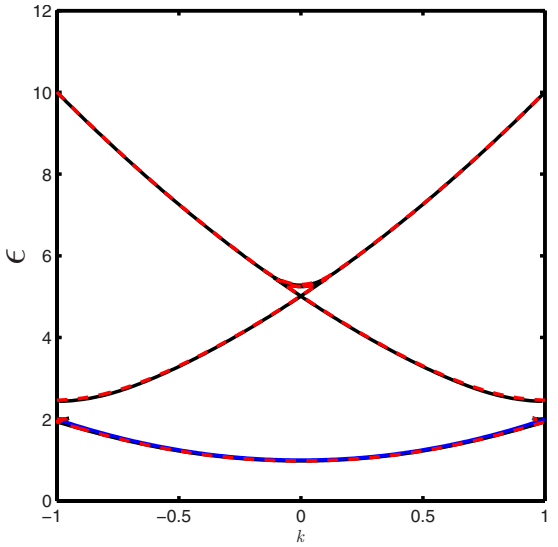

FIG. 1. (Color online) The band diagram with $V_0=1$, $\gamma=0.7377$ (rad), and $ng_{eff}=1$. The blue (lowest solid line), red (dashed lines), and black (upper solid lines) lines are calculated by 1-mode, 3-mode, and 5-mode, respectively. It shows that all the calculated results are close to each other when only the lowest three bands are considered.

~ 0 and $J(q_3)\sim 1/L_w^2$. The expression of $n_z(q_3)$ shows the dominant value at smaller values of q_3. Finally we obtain the effective one-dimensional equation for the dipolar BEC atoms in a quasi-one-dimensional optical lattice:

$$(\mu-\hbar\omega_\perp)\phi(z)=\left[-\frac{\hbar^2}{2m}\frac{d^2}{dz^2}+V_0\sin^2\left(\frac{\pi z}{d}\right)+\frac{N}{L_w^2}|\phi(z)|^2\left\{\frac{g_s}{2\pi}-\frac{2}{3}g_dP_2(\cos\gamma)\right\}\right]\phi(z), \tag{24}$$

where P_2 is the Legendre polynomial of the first kind. We arrived at the conclusion that with the approximated transverse part, the dipolar effects can be manipulated into an effective contact term with adjust parameter γ.

III. METHOD OF SOLUTION

In the previous section, we derived the effective Gross-Pitaevskii equation in Eq. (24) for condensate dipolar atoms in a quasi-one-dimensional lattice. In the following, we employ the many-mode expansion method for the Bloch functions to solve the corresponding energy band structures [5]. The energy functional of the effective one-dimensional system is

$$E[\phi]=\int_{\text{all sites}}\left[\frac{\hbar^2}{2m}\left|\frac{d\phi}{dz}\right|^2+V_0\sin^2\left(\frac{\pi z}{d}\right)|\phi(z)|^2+\frac{1}{2}\frac{1}{L_w^2}\left\{\frac{g_s}{2\pi}-\frac{2}{3}g_dP_2(\cos\gamma)\right\}|\phi(z)|^4\right]dz, \tag{25}$$

here we have defined

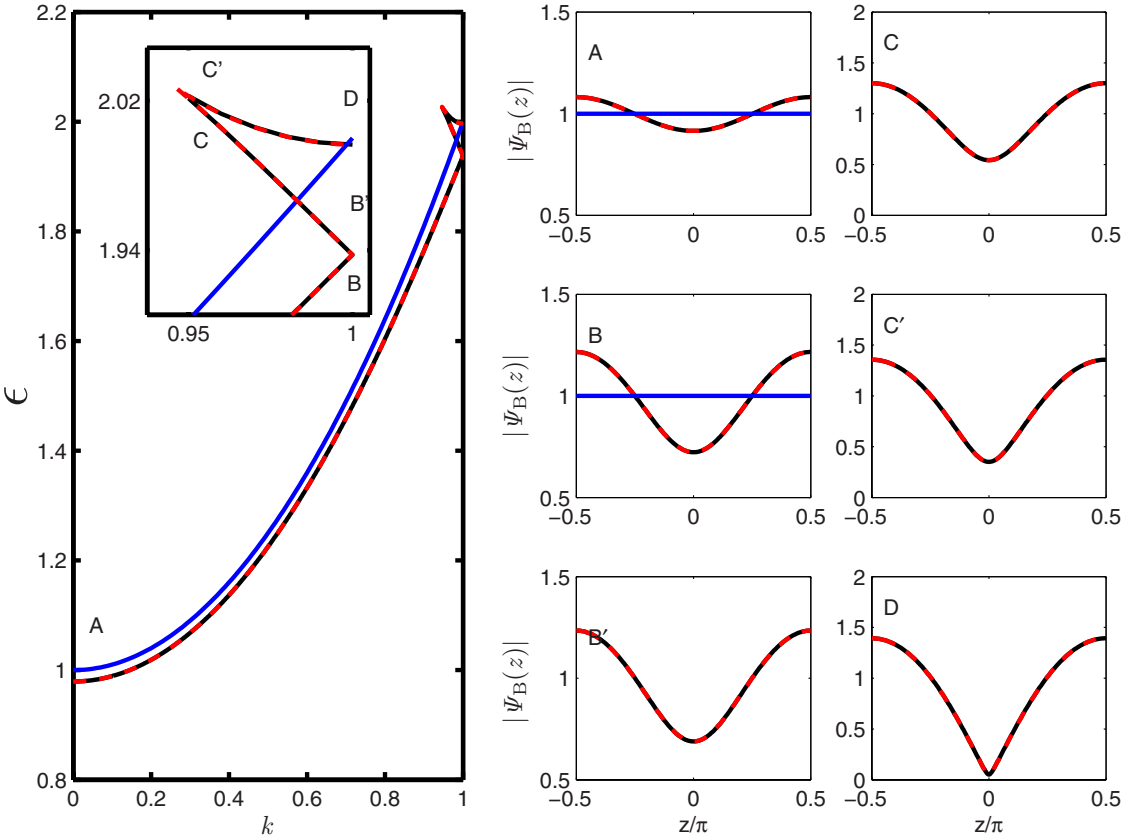

FIG. 2. (Color online) Part of the lowest band diagram with $V_0=1$, $\gamma=0.7377$ (rad), and $ng_{eff}=1$. The red dashed and black solid lines are derived from 3-mode and 5-mode models. The absolute value of the Bloch wave function of some interested modes is also plotted.

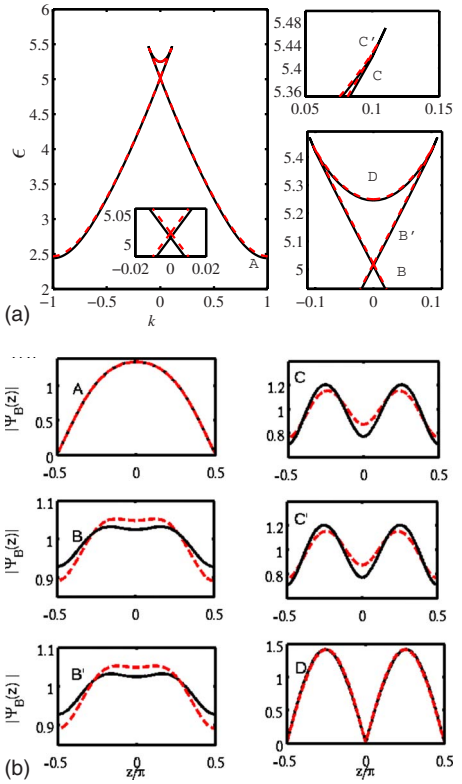

FIG. 3. (Color online) (a) Part of the first excited band diagram with $V_0=1$, $\gamma=0.7377$ (rad), and $ng_{eff}=1$. The red dashed and black solid lines are derived from 3-mode and 5-mode models. (b) The absolute value of the Bloch wave function of some interested modes is also plotted.

$$\int_{\text{all sites}} |\phi(z)|^2 dz = N. \tag{26}$$

In the following, we will use the recoiled energy $E_r = \pi^2\hbar^2/(2md^2)$ as the energy unit, and $L(=d/\pi)$ as the length unit. The unit cell is then $[-\pi/2, \pi/2]$ and the quasimomentum k lies in $[-1, 1]$. The energy density functional per site ϵ becomes

$$\epsilon[\phi] = \frac{1}{\pi}\int_{-(\pi/2)}^{\pi/2} \left[\left| \frac{d\phi}{dz} \right|^2 + V_0 \sin^2 z |\phi(z)|^2 + \frac{g_{eff}(\gamma)}{2} |\phi(z)|^4 \right] dz, \tag{27}$$

with the definition of number density per site

$$n = \frac{1}{\pi}\int_{-\pi/2}^{(\pi/2)} |\phi(z)|^2 dz, \tag{28}$$

where the effective coupling constant is

$$g_{eff}(\gamma) = \frac{1}{L_w^2 L E_r}\left\{ \frac{g_s}{2\pi} - \frac{2}{3} g_d P_2(\cos\gamma) \right\}. \tag{29}$$

In the many-mode method, the order parameter is written in the Bloch form:

$$\phi(z) = e^{ikz}\psi_B(z),$$

$$\psi_B(z+\pi) = \psi_B(z),$$

$$\psi_B(z) = \sqrt{n}\sum_{\mu} c_\mu e^{i2\mu z}. \tag{30}$$

The energy functional per atom can be recast as

$$\epsilon = \sum_{\nu} c_\nu^2 (k+2\nu)^2 + \frac{1}{2}V_0 - \frac{1}{4}V_0 \sum_{\nu} [c_\nu (c_{\nu+1} + c_{\nu-1})] + \frac{n}{2} g_{eff} \left[1 + \sum_{\mu,\nu}{}' \sum_{\mu',\nu'}{}' c_\mu c_\nu c_{\mu'} c_{\nu'} \delta_{\mu+\mu',\nu+\nu'} \right], \tag{31}$$

where in the double summations, we have $\mu \neq \nu$ and $\mu' \neq \nu'$, respectively. For a fixed number of modes in the Fourier expansion, the energy functional $\epsilon(k)$ is minimized with respect to the coefficients c_μ's for a given value of quasimomentum k.

For the numerical calculations, we assume that the optical lattice is constructed with lasers of wavelength 800 nm, and the lattice constant becomes $d=400$ nm. We are considering the chromium atoms with atomic magnetic dipole moment of 6 Bohr magneton, and trap frequency $\omega_\perp = 2\pi \times 712.5$ Hz from experimental parameters [11–14]. Thus the transverse length scale is $L_w = 0.523$ μm. With these parameters, we have

$$g_{eff}(\gamma) = 9.868 \times 10^{-5}(a/a_B) - 1.4913 \times 10^{-3} P_2(\cos\gamma), \tag{32}$$

where a_B is the Bohr radius. Note that even for the case of attractive contact interaction (negative scattering length), because $-0.5 \leqslant P_2(\cos\gamma) \leqslant 1$, it is possible to tune the angle γ between the aligned dipoles with cylindrical axis, such that the g_{eff} is positive for the appropriate value of scattering length, the system will still be stable. Physically it means that the dipole-dipole interaction is repulsive and overcomes the attractive contact interaction with the chosen value of γ, then the 3-body collisional loss induced collapse can be prevented. Also, we can tune the scattering length a and align

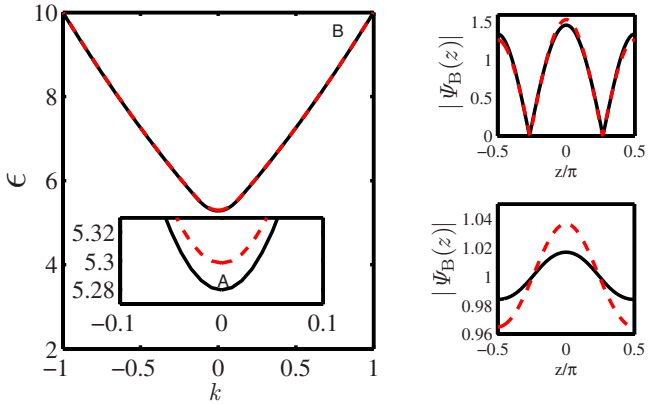

FIG. 4. (Color online) Part of the second excited band diagram with $V_0=1$, $\gamma=0.7377$ (rad), and $ng_{eff}=1$. The red dashed and black solid lines are derived from 3-mode and 5-mode models. The absolute value of the Bloch wave function of some interested modes is also plotted.

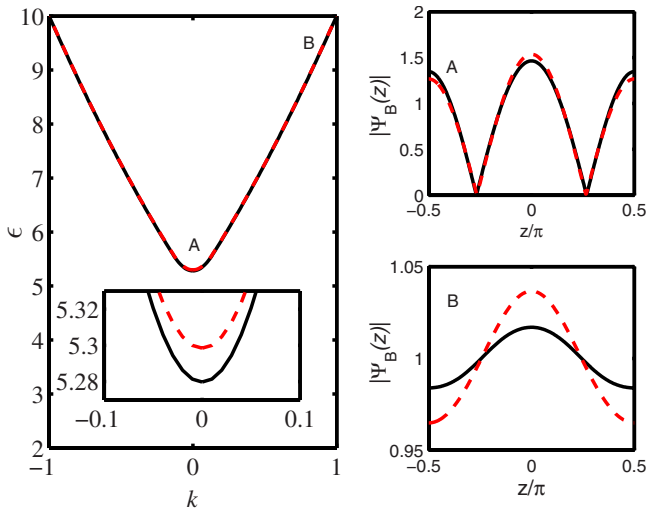

FIG. 5. (Color online) The band diagram with $V_0=1$ and $ng_{eff}=2$ derived from 3-mode models. Some amplitudes of the Bloch wave function are also plotted.

angle γ such that $g_{eff}\to 0$. The effects of contact interaction and dipole-dipole interaction will then cancel out each other such that the nonlinear effect has totally disappeared.

To show the properties of Bloch bands in dipolar lattices, we assume the scattering length a to be tuned by the Feshbach resonance technique to $a=15.1a_B$ such that the contact term and effective dipolar interaction are comparable to each other in our model. Thus our effective nonlinear coupling coefficient in the above equation becomes

$$g_{eff}(\gamma) = 1.4913 \times 10^{-3}[1 - P_2(\cos\gamma)]. \tag{33}$$

IV. RESULTS

We first calculate the three lowest band structures for $ng_{eff}=1$ and potential height $V_0=1$. The condition can be reached, for instance, with $n=1000$ and adjusting the alignment angle γ between the dipoles and the cylindrical axis to be 42.3°. Figure 1 depicts the energy bands calculated with 1-mode, 3-mode, and 5-mode expansions, respectively. We can see that the difference in results from the 1-mode, 3-mode, and 5-mode is very small. The swallow tail structure appears near the zone boundary of the ground band and near the zone center of the first excited band. Figure 2 shows more detailed results of the ground band. We can see that the 3-mode results show no swallow tail at the zone boundary. The calculation with at least 5-mode expansion is necessary. We plot also the amplitude of the Bloch wave function $|\psi_B(z)|$ for several interested values of wave number k. The use of absolute value is because the Bloch wave is in general complex. So, for a pure real or pure imaginary Bloch wave function, the particle current density, $j=\partial\epsilon(k)/\hbar\partial k$, vanishes. The Bloch wave amplitude at $k=0$ is designated as A. Near the zone boundary and with $k=0.99$, they are designated as B, B'. D corresponds to $k=1$, that is, at the zone boundary. Near the tip, they are designated as C and C'. Especially, at A and D, there is no particle current density.

Figure 3(a) shows the detailed structure of the first excited band near the zone center while in Fig. 3(b) we show the Bloch amplitudes. The swallow tail structure for the first excited band with $ng_{eff}=V_0=1$ appears only near the zone center instead of near the zone boundary as the ground band. The amplitude $|\psi_B(z)|$ at the zone boundary is designated as A. At the value of $k=0.01$, the Bloch amplitudes are designated as B and B', respectively. At the top of the band with $k=0$, the Bloch amplitude is designated as D; and near the tip, they are designated as C and C'. Again, the particle current density $j(k)$ for A and D vanishes.

In Fig. 4 we plot the detailed band structure of the second excited band and the corresponding Bloch amplitude for wave number at the zone center and the zone boundary. At

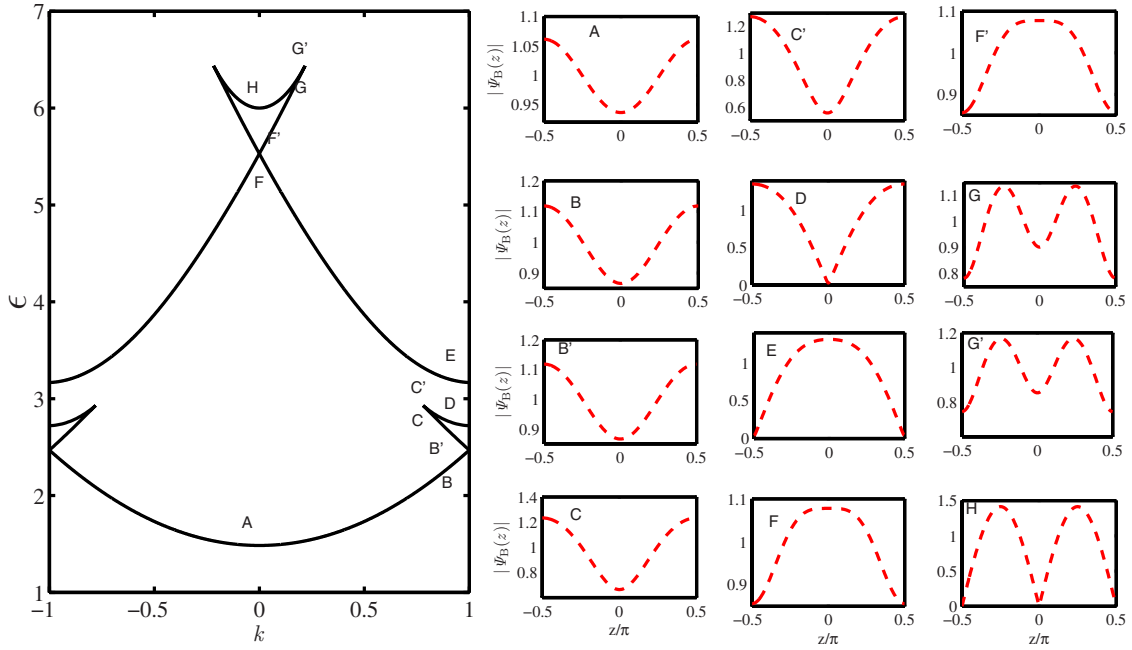

FIG. 6. (Color online) Part of the band diagram with $V_0=1$ and $ng_{eff}=2$ derived from 3-mode models. The absolute value of the Bloch wave function of some interested modes are also plotted.

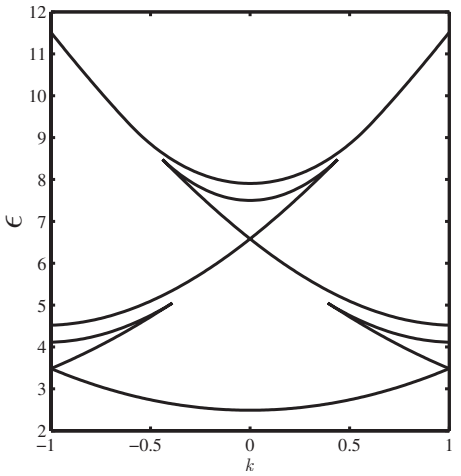

FIG. 7. The band diagram with $V_0=1$ and $ng_{eff}=4$ derived from 3-mode models.

this range of nonlinearity, the second excited band structure is not affected much. The property is similar to a Bloch electron in periodic potential. The Bloch wave at A, $k=0$, is a pure real function while at B, $k=1$, is a pure imaginary one.

In Fig. 5, the nonlinearity is increased to $ng_{eff}=2$ and the potential height is kept as $V_0=1$. We can see that the swallow tails of the ground and the first excited bands increased in size; but the second excited band still shows no special structure. We plot in Fig. 5 also the Bloch amplitude at the zone center and the zone boundary, designated as A and B, respectively. The two Bloch waves are purely real indicating that the particle current density vanishes. Figure 6 depicts the ground and the first excited band structure together with some interested Bloch amplitudes. For the ground band, A designates the zone center, B, B' are for the values of k slightly smaller than $k=1$ at the zone boundary. C and C' designate the places near the tip. D designates the top of the ground band at the zone boundary. For the first excited band, the swallow structure appears near the zone center. F and F' have values of $k=0.01$. G and G' are near the tip, and H designates the top of the first band at $k=0$. We further increase the nonlinearity to $ng_{eff}=4$ and keep the potential height in $V_0=1$. We can see that the swallow tail structures increase much in size as shown in Fig. 7.

V. DISCUSSION AND CONCLUSIONS

The realization of the dipolar BEC enables the study of an ultracold system with long-ranged interatomic interactions. We present in this work the study of the band structures of a dipolar BEC under quasi-one-dimensional lattices. In addition to the long-ranged interaction, we take into consideration the effects of transverse distributions mostly for BECs in quasi-one-dimensional lattice. We found that the dipole-dipole interaction and the transverse effects modify the effective coupling constant. The band diagrams of several values of nonlinear coupling constant and some interested mode are shown. On the other hand, the many-mode solution for a pure one-dimensional model has been studied in detail and not pursued repeatedly in this paper [6].

We found that the alignment angle between the dipoles and the axial direction provides a tunable parameter for physical properties through Eq. (33). The nonlinear effect, and hence the swallow tail in band structures, can be changed easily by adding a small magnetic field to adjust the alignment angle. From Eq. (32) of the effective coupling constant, even for the system with attractive mutual atomic interaction, it is still possible to adjust the alignment angle γ to obtain a positive value of g_{eff} such that the effective mutual interaction becomes repulsive to prevent collapse of the BEC system. It is also possible to adjust the value of γ such that the nonlinear effect vanished totally and reduced to an ordinary Bloch lattice.

In summary, due to the dipole-dipole interaction in the dipolar BEC in optical lattice, the system becomes versatile tunable. Comparing to the crystalline lattice in condensed matter physics, the dipolar BEC in an optical lattice will be an interesting system in band structure study. With such a tunable swallow-tailed loop in the band structures, interesting dynamics of the condensates between intraband and interbands are believed to be observed within current experimental technologies.

ACKNOWLEDGMENTS

The work of Y.Y.L. and R.K.L. was supported by the National Science Council of Taiwan under Contracts No. 95-2112-M-007-058-MY3 and No. NSC-95-2120-M-001-006. The work of T.F.J. was supported by the National Science Council of Taiwan under Contract No. NSC95-2112-M009-028-MY2. T.F.J. and Y.M.K. acknowledge the partial support from the Elite Foundation.

[1] O. Morsch and M. Oberthaler, Rev. Mod. Phys. **78**, 179 (2006).
[2] B. Wu and Q. Niu, Phys. Rev. A **61**, 023402 (2000).
[3] J. C. Bronski, L. D. Carr, B. Deconinck, and J. N. Kutz, Phys. Rev. Lett. **86**, 1402 (2001).
[4] J. C. Bronski, L. D. Carr, B. Deconinck, J. N. Kutz, and K. Promislow, Phys. Rev. E **63**, 036612 (2001).
[5] D. Diakonov, L. M. Jensen, C. J. Pethick, and H. Smith, Phys. Rev. A **66**, 013604 (2002).
[6] M. Machholm, C. J. Pethick, and H. Smith, Phys. Rev. A **67**, 053613 (2003).
[7] O. Zobay and B. M. Garraway, Phys. Rev. A **61**, 033603 (2000).
[8] K. Berg-Soresen and K. Molmer, Phys. Rev. A **58**, 1480 (1998).
[9] D.-I. Choi and Q. Niu, Phys. Rev. Lett. **82**, 2022 (1999).
[10] B. Wu and Q. Niu, Phys. Rev. A **64**, 061603(R) (2001).
[11] A. Griesmaier, J. Werner, S. Hensler, J. Stuhler, and T. Pfau,

Phys. Rev. Lett. **94**, 160401 (2005).
[12] J. Werner, A. Griesmaier, S. Hensler, J. Stuhler, T. Pfau, A. Simoni, and E. Tiesinga, Phys. Rev. Lett. **94**, 183201 (2005).
[13] J. Stuhler, A. Griesmaier, T. Koch, M. Fattori, T. Pfau, S. Giovanazzi, P. Pedri, and L. Santos, Phys. Rev. Lett. **95**, 150406 (2005).
[14] A. Griesmaier, J. Stuhler, and T. Pfau, Appl. Phys. B: Lasers Opt. **82**, 211 (2006).
[15] Q. Beaufils, R. Chicireanu, T. Zanon, B. Laburthe-Tolra, E. Maréchal, L. Vernac, J.-C. Keller, and O. Gorceix, Phys. Rev. A **77**, 061601(R) (2008).
[16] T. F. Jiang and W. C. Su, Phys. Rev. A **74**, 063602 (2006).
[17] Y. M. Kao and T. F. Jiang, Phys. Rev. A **75**, 033607 (2007).
[18] L. Santos, G. V. Shlyapnikov, P. Zoller, and M. Lewenstein, Phys. Rev. Lett. **85**, 1791 (2000).
[19] U. R. Fischer, Phys. Rev. A **73**, 031602(R) (2006).
[20] K. Gorál and L. Santos, Phys. Rev. A **66**, 023613 (2002).
[21] R. Citro, E. Orignac, S. De Palo, and M. L. Chiofalo, Phys. Rev. A **75**, 051602(R) (2007).
[22] A. S. Arkhipov, G. E. Astrakharchik, A. V. Belikov, and Yu. E. Lozovik, JETP Lett. **82**, 39 (2005).
[23] G. E. Astrakharchik and Yu. E. Lozovik, Phys. Rev. A **77**, 013404 (2008).
[24] G. E. Astrakharchik, J. Boronat, I. L. Kurbakov, and Yu. E. Lozovik, Phys. Rev. Lett. **98**, 060405 (2007).
[25] K. Gorál, L. Santos, and M. Lewenstein, Phys. Rev. Lett. **88**, 170406 (2002); M. Baranov, L. Dobrek, K. Gorál, L. Santos, and M. Lewenstein, Phys. Scr., T **T102**, 74 (2002).
[26] S. Yi, L. You, and H. Pu, Phys. Rev. Lett. **93**, 040403 (2004); L. Santos and T. Pfau, e-print arXiv:cond-mat/0510634.
[27] C. Kollath, Julia S. Meyer, and T. Giamarchi, Phys. Rev. Lett. **100**, 130403 (2008).
[28] H. Trompeter, W. Krolikowski, D. N. Neshev, A. S. Desyatnikov, A. A. Sukhorukov, Yu. S. Kivshar, T. Pertsch, U. Peschel, and F. Lederer, Phys. Rev. Lett. **96**, 053903 (2006).
[29] E. A. Ostrovskaya and Yu. S. Kivshar, Phys. Rev. Lett. **90**, 160407 (2003).
[30] T. Tsuzuki, J. Low Temp. Phys. **4**, 441 (1971).
[31] Z. Xu, Y. V. Kartashov, and L. Torner, Phys. Rev. Lett. **95**, 113901 (2005).
[32] Y. Y. Lin, I.-H. Chen, and R.-K. Lee, J. Opt. A, Pure Appl. Opt. **10**, 044017 (2008).
[33] A. Smerzi and A. Trombettoni, Phys. Rev. A **68**, 023613 (2003).
[34] A. Smerzi and A. Trombettoni, Chaos **13**, 766 (2003).